

## First Synthesis of Zeolite-encapsulated Copper(II)hydrazone Complex: Characterization and CO adsorption

Ayman H. Ahmed

Department of Chemistry, Faculty of Science, Al-Azhar University, Nasr City, Cairo, Egypt.

**Abstract:** Copper (II) complex of salicylidinebenzenesulphonylhydrazone ligand (SBSH) encapsulated in Y-zeolite was synthesized by a diffusion method, and its catalytic efficiency toward CO adsorption was examined by in-situ FT-IR spectroscopy. The results obtained were investigated and compared with that of the related metal exchanged zeolite. The prepared zeolites were characterized by a battery of techniques: elemental analysis, FT-IR, UV-Visible, magnetic susceptibility as well as XRD pattern. Additionally, N<sub>2</sub> - adsorption studies and thermal analysis (TG, DTG and DTA) have provided further evidence for the intrazeolite location of the metal complex. Conversion of CO into CO<sub>2</sub> was evidenced by the in-situ FT-IR of CO adsorption on Cu<sup>II</sup>-Y and Cu<sup>II</sup>(SBSH)/Y samples. The data revealed that, Cu<sup>II</sup>(SBSH)/Y is an active material for CO adsorption under different conditions in contrast to Cu<sup>II</sup>-Y. The higher reactivity of CO chemisorption for Cu<sup>II</sup>(SBSH)/Y can be attributed to the higher density of positive charges in the cationic copper complex compared to that in Cu<sup>II</sup>-Y.

**Keyword:** Zeolite encapsulated Cu<sup>II</sup> -hydrazone complexes; Diffusion method

### INTRODUCTION

Encapsulation of suitable molecular species in zeolitic cavities to prepare new type of functional materials has been a popular field of study<sup>[1,5]</sup>. The prepared materials can have many interesting applications including chromatropism, size / shape-selective catalysis, gas separation / purification, electro and photocatalysis, etc.<sup>[6,8]</sup>. Basically, there have been two main approaches to prepare zeolite-encapsulated complexes, namely the zeolite synthesis (ZS)<sup>[9]</sup> and flexible ligand (FL)<sup>[10,14]</sup> methods. In the FL method that used in this work, a flexible ligand, able to diffuse freely through the zeolite pores, coordinates with a previously exchanged metal ion. Upon complexation, the resulting complex becomes too large and rigid to escape from the cage. Recently, metal complex of porphyrins, phthalocyanines, Schiff bases and some amines, etc. have been encapsulated into zeolite matrix for the development of efficient biomimetic oxidation catalysts which have acted as the functional mimic of metalloenzymes<sup>[15,19]</sup>. Zeolite complexes possess a number of structural similarities to metalloenzymes and therefore they are expected to mimic enzyme active sites for the catalytic reaction such as oxidation<sup>[14]</sup>, hydrogenation<sup>[20]</sup>, dehalogenation<sup>[21]</sup>, etc. The CO adsorption may be particularly relevant because it is an unwanted product

(air pollutant) and/or a key intermediate of many reactions. So, adsorption and oxidation of CO is considered to be an environmental target. Adsorption of CO is one of the most useful methods for characterizing the nature of introduced metal ions in zeolites, it had not been used for zeolite encapsulated complexes of copper (II) with hydrazone yet.

In the present paper, we report the synthetic, physicochemical characterization and CO adsorption of encapsulated copper (II) complex with a type of hydrazone ligand (first to use in encapsulation process with exchanged copper ion) derived from salicyaldelyde and benzenesulphonyldrazide. The resulting material is considered a new material and may be used to grow up numbers of heterogeneous catalysts. Surface properties and physical adsorption of nitrogen were also studied to describe the texture of these composite solid materials and provide further evidence for the immobilization of the metal complex within the zeolite cavities.

### MATERIALS AND METHODS

All the chemicals used in this work were of Aldrich or Analar grade quality. NaY zeolite (Lot No. D1-9915, HSZ - 320N - NAA, Si/Al=5.6) was obtained from Toyota Company Ltd., Japan and used as a host matrix. The metal content was determined by

**Table 1:** Physical and analytical data as well as surface characteristics for SBSH, NaY and the prepared zeolites.

Sample label	Colour	M%	M.p	M/C ratio Found(calcd.)	$\gamma$ , (c.g.s.)	$S_{\text{NET}}$ (m <sup>2</sup> /g)	$S$ , (m <sup>2</sup> /g)	$V_p$ (cm <sup>3</sup> /g)
SBSH	White	-	155	-	-	-	-	-
NaY	White	-	-	-	Diamag.	873	860	0.80
Cu <sup>II</sup> -Y	Pale blue	6.80	>300	-	$0.114 \times 10^{-5}$	633	603	0.63
Cu <sup>II</sup> (SBSH)/Y	red	7.01	>300	0.225(0.231)	$0.048 \times 10^{-5}$	481	466	0.35

complexometric titration with EDTA using xylenol orange indicator, hexamine buffer and sodium fluoride as a masking agent for the interfering aluminium ions result from disintegration of the zeolite framework<sup>[22]</sup>. The results obtained were confirmed by using Varian atomic absorption spectrometer (Varian-AA220). Elemental analysis was determined by microanalyses, Table 1. IR spectra were recorded as KBr pellet in the range 200 - 4000 cm<sup>-1</sup> on a Mattson 5000 FT-IR spectrometer. Electronic spectra were recorded in Nujol mull using a Perkin-Elmer lambda 35 UV/Vis. spectrophotometer. The mass susceptibility<sup>[23]</sup> was measured at room temperature using magnetic susceptibility balance of models Johnson metthey and Sherwood. X- ray diffractograms of the solid zeolite samples were recorded with PW 1840 Philips diffractometer (Cu K $\alpha$  used as target). The thermal analysis (TG, DTG, DTA) were carried out for Cu<sup>II</sup>(SBSH)/Y catalyst with a Shimadzu thermal analyzer model 50 H. FT-IR spectra of CO adsorbed on the prepared catalysts were recorded by using FT-IR instrument Bruker (Vector 22) single beam spectrometer with a resolution of 2 cm<sup>-1</sup>. The self-supporting wafer of about 30 mg cm<sup>-2</sup> was placed in an in-situ FT-IR cell equipped with a build-in furnace and thermally evacuated at 200°C under a reduced pressure 10<sup>-5</sup> Torr for 1 h before admitting 50 Torr of CO at room temperature. The cell was allowed to equilibrate for 20 min and, then, evacuated at room temperature (RT), 50 and 100 °C respectively. At each step, the FT-IR spectrum was recorded after cooling down to room temperature. The free CO spectrum was subtracted from the spectrum recorded in each step.

**Preparation of Ligand:** The hydrazone ligand used is salicylidinebenzenesulphonylhydrazone (SBSH) and has the structural formula shown in Fig. 1. It was prepared using the procedure reported in the literature<sup>[24]</sup> (m.p=155, lit. m.p=155 °C). The ligand structure has been confirmed by FT-IR spectroscopy and its purity was checked by mass spectrometry. The mass spectrum of the free ligand revealed a molecular ion peak (M<sup>+</sup> value) at m/z = 276; Cald. = 276.3<sup>[25]</sup>.

**Preparation of Cu<sup>II</sup>-Y:** The Cu<sup>II</sup>-Y sample was prepared by using the same procedure described in

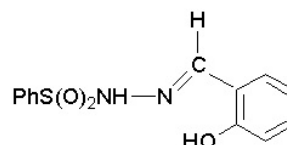


**Fig. 1:** SBSH

literature<sup>[26]</sup> as follows. An amount of 7.0 g NaY zeolite was treated at room temperature with 1500 ml 0.01M acetate solution of Cu(II) ion. The mixture was conducted for 48 h with continuous stirring. After the exchanging was completed, the zeolite sample was filtered off, washed thoroughly with distilled water to remove the excess of unreacted ions till the filtrate was free from any copper ion content. The zeolite sample was then dried for 24 h in air at room temperature and finally stored over saturated ammonium chloride solution (to maintain a constant humidity) until required for use [exchange level = 74.4 %].

**Preparation of Zeolite Encapsulated Cu<sup>II</sup>-complex:** For the preparation of Cu<sup>II</sup>(SBSH)/Y, Approximately 1.0 g of Cu<sup>II</sup>-Y was activated at 200 °C under a vacuum of 10<sup>-4</sup> Torr for 2 h and then cooled to room temperature. This activated material was thoroughly mixed with an excess of SBSH (2.0 g) in a glove bag under nitrogen atmosphere. The finely powdered mixture was placed horizontally in a Pyrex shrink tube, evacuated again to 10<sup>-4</sup> Torr for 10 min. and heated with constant stirring at 135 °C for 4 h. After the reaction was completed whereby the ligand diffuses freely through the channels and coordinates with metal ions, the furnace tube was cooled to room temperature, carefully opened and the products were washed in a beaker with successive portions of hot solvents (ethanol, acetone and methylene chloride, respectively). The product sample was then Soxhlet – extracted with ethanol for 48 h at normal conditions to remove the excess of unreacted (SBSH) and finally dried for 4 h at 100 °C in oven.

## RESULTS AND DISCUSSIONS

**IR spectra:** In comparison to NaY zeolite, It was noticed that the IR spectra of Cu<sup>II</sup>-Y and Cu<sup>II</sup>(SBSH)/Y are dominated by the Y zeolite bands assignable to

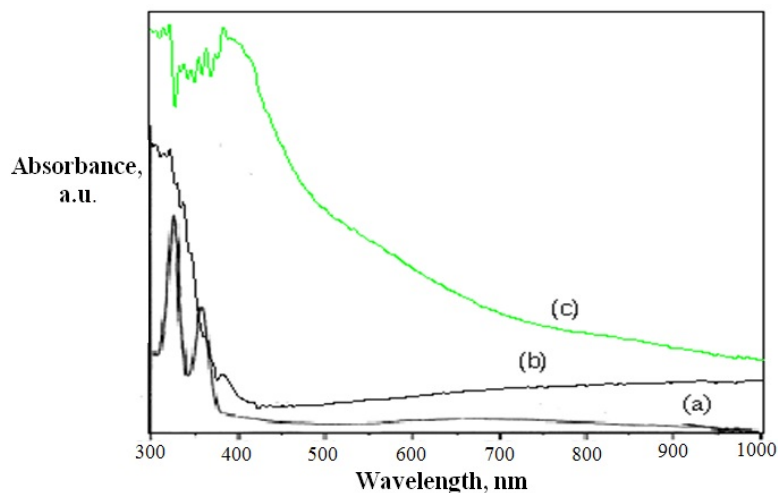


**Fig. 2:** UV-Vis. spectra of (a) Cu<sup>II</sup>-Y, (b)SBSH (c) Cu<sup>II</sup>(SBSH)/Y.

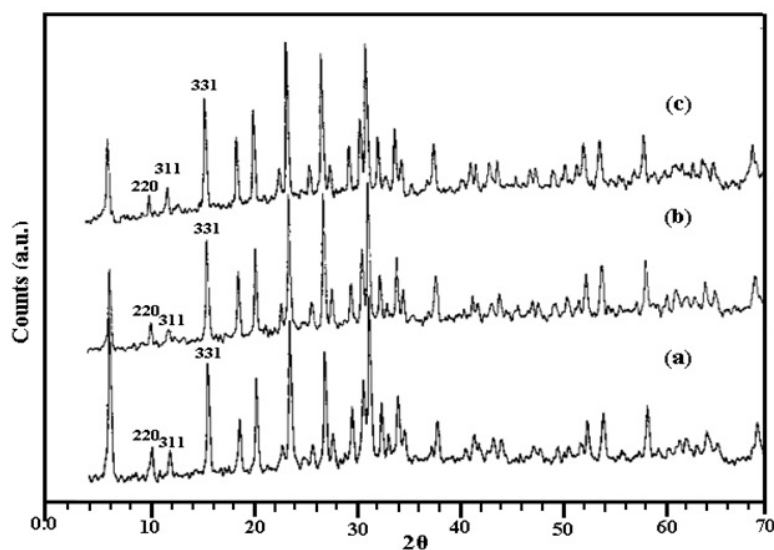


**Fig. 3:** X-ray powder diffraction patterns of (a) NaY, (b) Cu<sup>II</sup>-Y and (c) Cu<sup>II</sup>(SBSH)/Y.

surface hydroxyl groups, internal and external vibrations of tetrahedral geometry of the type (Si,Al)O<sub>4</sub> without any collapse in their crystallinity. No change in the shapes or positions of zeolite structure - sensitive vibrations was observed upon inclusion the metal ion or its complex that result in dealumination or distortion<sup>[26]</sup>. The infrared spectra of Cu<sup>II</sup>-Y and Cu<sup>II</sup>(SBSH)/Y showed a new band at 1400 cm<sup>-1</sup> assignable to δOH (in plane) referring to the presence of coordinated water<sup>[27]</sup>. Comparing the IR spectra of the free (SBSH) ligand reported in literature<sup>[25]</sup> with that of Cu<sup>II</sup>(SBSH)/Y within the window of 1200 - 1600 cm<sup>-1</sup> disclosed the following upon complexation. (1) ν<sub>as</sub>(SO<sub>2</sub>) group of the ligand was shifted to high and appeared at 1348 cm<sup>-1</sup> suggesting the involvement of

this group in complexation (2) δ(OH)phenolic and δ(NH) disappeared indicating the deprotonation of such groups (3) ν(C=N) of the SBSH overlapped with the band attributed to the adsorbed water at 1636 cm<sup>-1</sup> as observed from the broadening of this band indicating the involvement of this group in coordination. Those observations not only confirm the formation of Cu<sup>II</sup>(SBSH) complex inside the zeolite, but also suggest that its structure differentiates to a large extent than that obtained by traditional methods<sup>[24]</sup>.

**Electronic Spectra and Magnetic Properties:** The electronic spectrum of Cu<sup>II</sup>-Y (Fig. 2) showed a broad band centered at 670 nm assigned to <sup>2</sup>E<sub>g</sub> - <sup>2</sup>T<sub>2g</sub> transition in a tetragonal-distorted octahedral around the

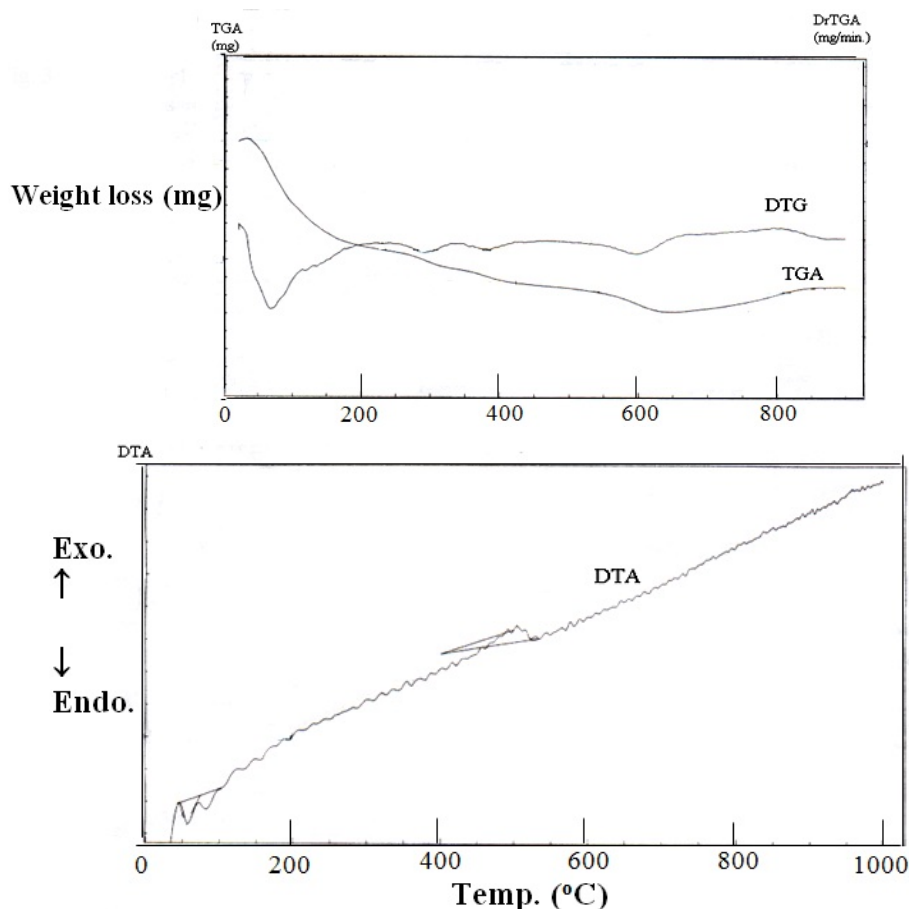


**Fig. 4:** TGA, DTG and DTA of  $\text{Cu}^{\text{II}}(\text{SBSH})/\text{Y}$ .

$\text{Cu}^{\text{II}}$  ion<sup>[26,28]</sup> while  $\text{Cu}^{\text{II}}(\text{SBSH})/\text{Y}$  showed an absorption band at 834 nm (Fig. 1) suggesting a pseudo tetrahedral configuration around the  $\text{Cu}(\text{II})$  ion and a band at 535 nm due to  $\text{L} \rightarrow \text{Cu}$  charge – transfer<sup>[28]</sup>. This indicates that the  $\text{Cu}^{\text{II}}$  ions changed their configuration upon chelation confirming the formation of the complex.

The very low paramagnetic value of  $\chi_g$  for  $\text{Cu}^{\text{II}}(\text{SBSH})/\text{Y}$  (Table 1) indicates that the  $\text{Cu}(\text{II})$  ions are close to each other. The  $\text{Cu} - \text{Cu}$  interaction gives rise to incomplete quenching of the spin moments of the ions. This means that the supposition of three copper ions in the molecular structure is not excluded and the obtained value of  $\chi_g$  agrees to a great extent with the proposed structure.

On the basis of the elemental analyses (Table 1), magnetism, and spectral (IR and UV-Vis.) data for the zeolite samples under investigation, the most probable structures of  $\text{Cu}(\text{II})$  ions inside Y zeolite for  $\text{Cu}^{\text{II}}-\text{Y}$  and  $\text{Cu}^{\text{II}}(\text{SBSH})/\text{Y}$  are represented by structure I, II respectively.

**XRD:** X-ray diffraction exhibits that the crystallinity and morphology of zeolite Y is preserved in spite of the inclusion of the  $\text{Cu}(\text{II})$  ions or its complex (Fig. 3). This result is in good agreement with IR results obtained previously. Diffraction characteristic feature for any new phase in the diffractograms was not detected. From a comparison of patterns (a) with (b) it may be seen that little changed occurred in the relative intensities of the 331, 311 and 220 peaks upon introducing of exchanged metal ions. This means that the zeolite lattice retained its originally random sodium ion distribution after the exchanging process. In contrast, analysis of the patterns for the encapsulated complex indicated that significant cation redistribution occurred following complex formation within the zeolite supercages<sup>[26,29]</sup>. It is suggested that the formation of large  $\text{Cu}^{\text{II}}(\text{SBSH})/\text{Y}$  complex leads to disturb the random distribution of small extra framework cations. This change in location of small cations affects the relative intensities of 331, 311 and 220 peaks. Indeed, XRD clearly showed that the large complex displaced sodium ions from their random

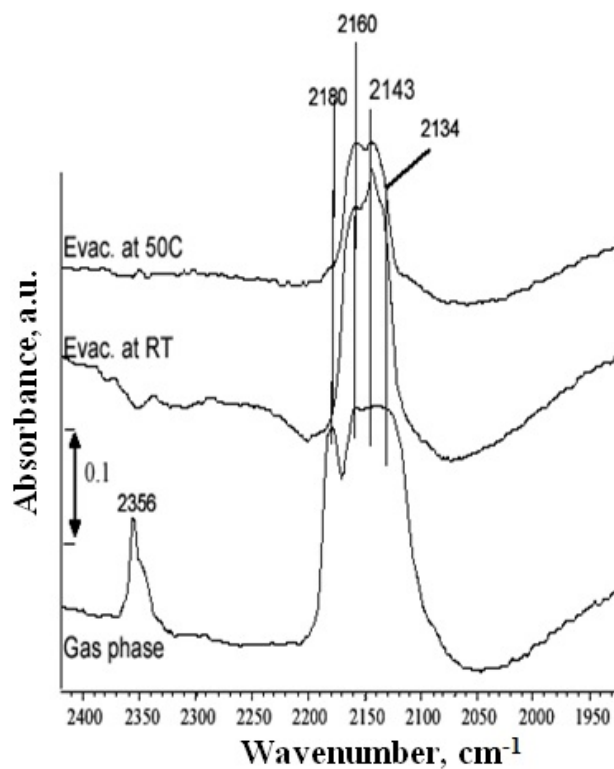


Fig. 5: In-situ FT-IR spectra of CO adsorbed on Cu<sup>II</sup>-Y.

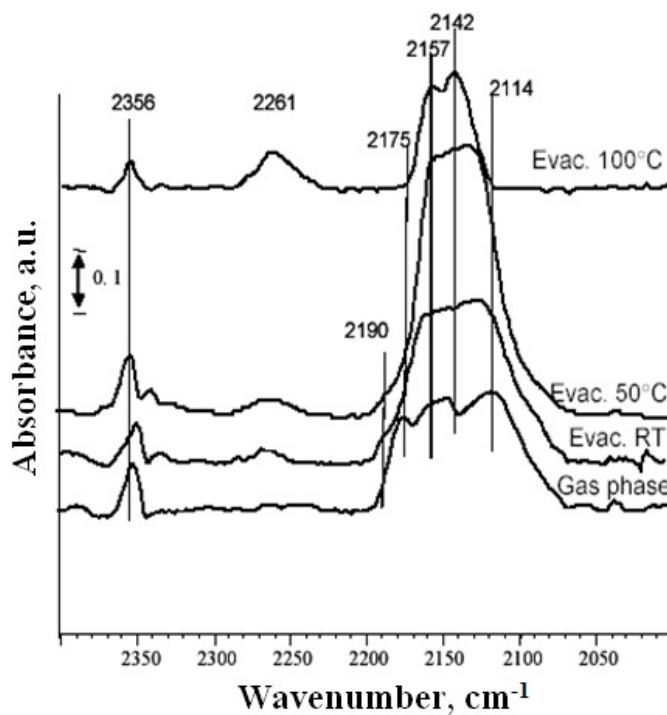


Fig. 6: In-situ FT-IR spectra of CO adsorbed on Cu<sup>II</sup>(SBSH)/Y.

positions in the supercages to locations at sites II (located at the center of a single six-ring, S6R), I' (located in the sodalite cavity) and are placed inside the cages of zeolite Y.

**Thermal Studies:** The TG thermogram of Cu<sup>II</sup>(SBSH)/Y (Fig. 4) showed two stages of decomposition starting at 37 and 232 °C due to the desorption of water from the voids of zeolite sample. On the other hand, the DTA pattern (Fig. 4) showed two peaks located at 57 and 504 °C. The former is endothermic peak accompanied by weight loss referring to the removal of water from zeolite while the latter is exothermic peak accompanied by weight loss (as in TG curve) and is most probably due to the thermal decomposition of the encapsulated copper complex. The results indicate that the encapsulated complex stable up to 533 °C. Worthy to mention that the reported Cu<sup>II</sup>-SBSH complex formed under ordinary conditions is decomposed at 290 °C<sup>[25]</sup>. This undoubtedly indicates that the formation of the complex inside the zeolite cages enable us to prepare analogous complex not only with different structure but also with high thermal stability.

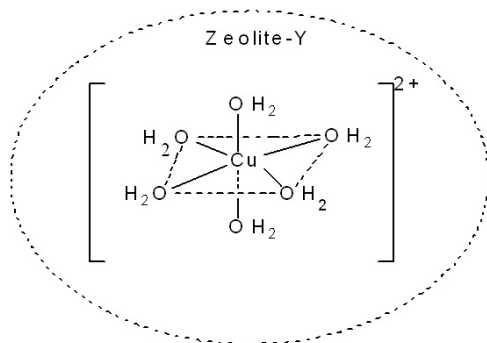
**Surface Characteristics:** The nitrogen adsorption-desorption isotherms for Cu<sup>II</sup>-Y and Cu<sup>II</sup>(SBSH)/Y sample appeared as isotherm belongs to type II of Brunauer's classification<sup>[30]</sup> with a small hysteresis loops of different shapes and areas at relative vapour pressure  $p/p^\circ$  of 0.17 - 0.95. The presence of this loop indicates the porous nature of these solids. Isotherm of Cu<sup>II</sup>(SBSH)/Y showed a very weak hysteresis loop with a decrease in the N<sub>2</sub> - adsorbed amount compared with that of Cu<sup>II</sup>-Y indicating the filling of the zeolite pores by the complex and the existence of complex inside the zeolite cavities not on the surface. The surface area ( $S_{BET}$ ) and pore volume values were identified and given in Table 1. There is a drastic reduction of surface area and pore volume of zeolites upon introducing of the metal ion or its corresponding metal complex. Since the zeolite framework structure is not affected by encapsulation as shown from the IR spectra and XRD pattern, the reduction of surface area and pore volume provides an additional evidence for the presence of complex inside the cavities and refers to the degree of filling for these cavities. The specific surface area ( $S_p$ ) for these catalysts were determined from the  $V_{1-t}$  plots and are vary close to ( $S_{BET}$ ) indicating the correct choice of the standard t-curves. The obtained  $V_{1-t}$  plot of Cu<sup>II</sup>(SBSH)/Y showed downward deviation, indicating the domination of narrow pores due to the filling of zeolite supercages by the formed Cu(II) complex whereas the  $V_{1-t}$  plot of

Cu<sup>II</sup>-Y showed an upward deviation indicating the domination of wide pores owing to the creation of new pores by exchanging process.

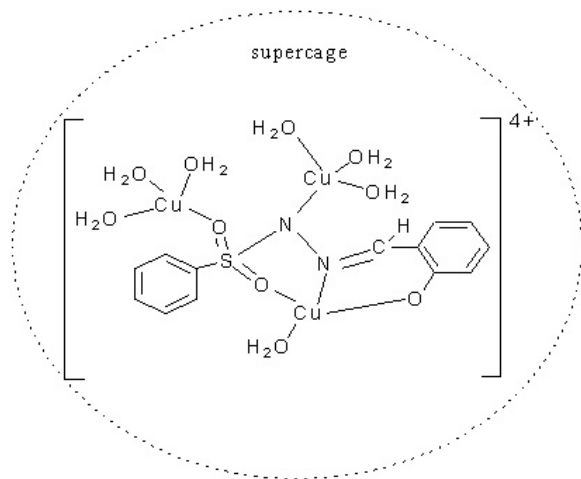
**CO adsorption:** CO gas was adsorbed on NaY exchanged Cu<sup>II</sup> and NaY encapsulated Cu<sup>II</sup> -complex. The changes were persuaded using in-situ FT-IR in the range of (C=O) carbonylic region (2000- 2400 cm<sup>-1</sup>). It was difficult to detect and stabilize Cu<sup>II</sup> ions at room temperature (RT) during the adsorption of CO<sup>[31,33]</sup>. CO is strongly adsorbed on Cu(I) ions since the carbonyls formed are stabilized by  $\pi$  - back - donation<sup>[34,36]</sup>.

**CO Adsorbed on Cu<sup>II</sup>-Y Catalyst:** As presented in previous paper<sup>[26]</sup>, The CO adsorption at room temperature onto thermally evacuated Cu<sup>II</sup>-Y at 200 °C (Fig. 5) leads to develop absorption bands at 2356 and 2180 cm<sup>-1</sup> assigned to C-O stretching mode of adsorbed CO<sub>2</sub> and geminal Cu<sup>I</sup>-(CO)<sub>2</sub>, respectively<sup>[37-39]</sup>. The presence of CO as a reducing agent leads to the generation of a certain amount of Cu(I) ions. The growth of CO<sub>2</sub> band at 2356 cm<sup>-1</sup> is likely occurred due to water gas shift reaction (WGS), which is proceeded as a result of CO interaction with residual of water molecules in zeolite. A broad peak around 2200 - 2160 cm<sup>-1</sup> was developed which is tentatively assigned to physically adsorbed and H-bonded CO under equilibrium CO pressure. Evacuation at room temperature removes the 2356 and 2180 cm<sup>-1</sup> bands. The geminal Cu<sup>I</sup>-(CO)<sub>2</sub> band (2180 cm<sup>-1</sup>) has been documented only at equilibrium CO pressure<sup>[40]</sup>. Simultaneously, the broad band (2200 - 2160 cm<sup>-1</sup>) was resolved partially to 2160, 2143 and 2134 cm<sup>-1</sup> bands. The bands at 2160 and 2143 cm<sup>-1</sup> are due to a  $\nu$ (CO) stretching in Cu<sup>I</sup>-CO species, which are consistent with literature data<sup>[40,41]</sup>. The presence of different Cu<sup>I</sup>-CO species points to different environments around Cu<sup>I</sup> species. Thermal evacuation at 50 °C for 30 min led to the overall bands decrease in intensity.

**CO adsorbed on Cu<sup>II</sup>(SBSH)/Y catalyst:** IR spectra of CO adsorbed on Cu<sup>II</sup>(SBSH)/Y complex, Fig. 6, produced vibrational spectra with a band at 2356 cm<sup>-1</sup> assigned to free CO<sub>2</sub>, 2175 cm<sup>-1</sup> assigned to geminal Cu<sup>I</sup>-(CO)<sub>2</sub> and a broad bands within 2070 - 2165 cm<sup>-1</sup> region. The last band may be resolved into a group of bands around 2157, 2142 and 2114 cm<sup>-1</sup> point to the presence of three kinds of linear Cu(I)-CO in zeolite. This may be explained on the basis that the Cu(II) of the encapsulated complex was reduced by CO into Cu(I) and the water molecules proposed in its structure II were replaced by CO giving three kinds of terminal



**STRUCTURE I**



**STRUCTURE II**

CO groups. By evacuation, it is noticed that the band at  $2175\text{ cm}^{-1}$  disappeared while the intensity of the  $2157$ ,  $2142$  and  $2114\text{ cm}^{-1}$  increases up to  $50\text{ }^{\circ}\text{C}$ . This indicates that the CO of thermally unstable geminal  $\text{Cu}^{\text{I}}-(\text{CO})_2$  became free and made a reduction for  $\text{Cu}^{\text{II}}$  ions in another part of unreduced encapsulated  $\text{Cu}^{\text{II}}(\text{SBSH})$  complex to  $\text{Cu}(\text{I})$  forming new  $\text{Cu}(\text{I})-\text{CO}$  bonds. The decrease in intensity of these resolved bands with thermal evacuation at  $100\text{ }^{\circ}\text{C}$  indicates the disruption of  $\text{Cu}(\text{I})-\text{CO}$  bonds. The band at  $2261\text{ cm}^{-1}$  is most probably due to the adsorption of  $\text{CO}_2$  on  $\text{Cu}^{2+}$  ions belong to the complex<sup>[42]</sup>. From preceding data, it can be said that CO was converted to  $\text{CO}_2$  on the surface of  $\text{Cu}^{\text{II}}(\text{SBSH})/\text{Y}$  probably by coordinated or intracrystalline  $\text{H}_2\text{O}$  molecules in zeolite i.e. water gas shift reaction (WGSR) was occurred or by the effect of oxygen zeolite lattice under different circumstances. This suggestion is supposed on the basis of the still appearance of free  $\text{CO}_2$  bands in all steps in contrast to  $\text{Cu}^{\text{II}}-\text{Y}$  which showed a CO adsorption only in the gas phase step.

In summary, the results showed that  $\text{Cu}^{\text{II}}(\text{SBSH})/\text{Y}$  can be isolated by using a diffusion method and  $\text{Cu}(\text{II})$  ions of the occluded complex coordinate to the hydrazone ligand to give 3:1 metal - ligand complex with a distorted tetrahedral geometry. The different Physico- chemical studies on the prepared  $\text{Cu}^{\text{II}}(\text{SBSH})/\text{Y}$  showed that the composition and structure of the encapsulated complex differ to a large extent from that of free one prepared by traditional method. The distortion in the structure of the prepared immobilized complex and its deviation from the known solution chemistry is expected because of spatial constraints imposed by the dimensions of the zeolite cage. Oxidation of CO forming  $\text{CO}_2$  may be evidenced by the in-situ FT-IR spectroscopy and the data revealed that,  $\text{Cu}^{\text{II}}(\text{SBSH})/\text{Y}$  is an active material for CO adsorption under numerous conditions meanwhile  $\text{Cu}^{\text{II}}-\text{Y}$  makes CO adsorption only in the gas phase due to the CO interaction with crystalline water molecules of zeolite (WGSR).

## REFERENCES

- (a) Cuzman, J., B.C. Gates, 2003. *J. Chem. Soc. Dalton Trans.*, 3303, and references therein. (b) Ganesan, R., B. Viswanathan, 2004. *J. Phys. Chem. B.*, 108: 7102.
- Borja, M., P.K. Dutta, 1993. *Nature.*, 362: 42.
- Thomas, J.M., 1999. *Angew. Chem. Int. Edit. Engl.*, 38: 3588.
- Zsigmond, A., K. Bogar and F. Notheisz, 2003. *J. Catal.*, 213: 103.
- Ramamurthy, V., D.R. Sanderson and D.F. Eaton, 1993. *J. Am. Chem. Soc.*, 115: 10438.
- Ramamurthy, V., P. Lakshminarasimhan, C.P. Grey and L.J. Johnston, 1998. *Chem. Commun.*, 2411, and refernces therein.
- Meinershagen, J.L., T. Bein, 1999. *J. Am. Chem. Soc.*, 121: 448.
- Sykora, M., K. Maruszewski, S.M. Treffert – Ziemelis and J.R. Kincaid, 1998. *J. Am. Chem. Soc.*, 120: 3490.
- Balkus Jr., K.J., A.G. Gabrielov and S. Bell, 1994. *Inorg. Chem.*, 33: 67.
- Bowers, C., P.K. Dutta, 1990. *J. Catal.*, 122: 271.
- Herron, N., 1986. *Inorg. Chem.*, 25: 4714.
- Balkus Jr., K.J., A.A. Welch and B.E. Gnade, 1990. *Zeolites.*, 10: 722.
- Kowalak, S., R.C. Weiss and K.J. Balkus Jr. 1991. *J. Chem. Soc. Chem. Commun.*, 57.
- Balkus Jr., K.I., A.G. Gabrielov, 1995. *J. Inclus. Phenom. Molec. Recog. Chem.*, 21: 159.

15. Bedioui, F., 1995. *Coord. Chem. Rev.*, 144: 39.
16. Saha, P.K., S. Banerjee, S. Saha, A.K. Mukherjee, S. Sivasanker and S. Koner, 2004. *Bull. Chem. Soc., Jpn.*, 77: 709.
17. Weckhuysen, B.M., A. Verberckmoes, I.P. Vannijvel, J.A. Pelgrims, P.L. Buskens, P.A. Jacobs and R.A. Schoonheydt, 1995. *Angrew. Chem. Int. Edit. Engl.*, 34: 2652.
18. Koner, S., 1998. *Chem. Commun.*, 593.
19. Tolman, C.A., J.D. Droliner, M.J. Nappa and N. Herron, 1989. *Activation and Functionalisation of Alkanes*, in: CL Hill (ED), Wiley, Chichester, pp: 303.
20. Chatterjee, D., H.C. Bajaj, A. Das and K. Bhatt, 1994. *J. Mol. Catal.*, 92: 235.
21. Raja, R., P. Patnaswamy, 1997. *J. Catal.*, 170: 244.
22. Vogel, A.I., 1989. *A text Book of Quantitative Inorganic Analysis*, Longman (5th ed.), London.
23. Szafran, Z., R.M. Pike and M.M. Singh, 1991. *Microscale Inorganic Chemistry*, John Wiley, New York.
24. Rakha, T.H., M.M. Bekheit and K.M. Ibrahim, 1992. *Transition Met. Chem.*, 17: 517.
25. Ahmed, A.H., 2007. *J. Mol. Stuct.*, 839: 18.
26. Salama, T.M., A.H. Ahmed and Z.M. El-Bahy, 2006. *Micropor. Mesopor. Mater.*, 89: 251.
27. Ewing, W.G., 1975. *Instrumental Methods of Chemical Analysis* (4th ed.), McGraw – Hill Kogakusha, 1975, Vogel, A.I., 1975. *A Text Book of Practical Organic Chem.* (3rd ed.), Longman, pp: 704.
28. Lever, A.B.P., 1968. *Inorganic Electronic Spectroscopy*, Elsevier Publishing Company, Amsterdam.
29. Quayle, W.H., J.H. Lunsford, *Inorg. Chem.*, 21: 2226.
30. Brunauer, S., L.S. Deming, W.S. Deming and E. Teller, 1940. *J. Am. Chem. Soc.*, 62: 1723.
31. Kantcheva, M., K. Hadjiivanov, A. Budneva and A. Davydov, 1992. *Appl. Surf. Sci.*, 55: 49.
32. Busca, B., 1987. *J. Mol. Catal.*, 43: 225.
33. Davydov, A., 1984. *IR Spectroscopy Applied to Surface Chemistry of Oxides*, Nauka, Novosibirsk.
34. Hadjiivanov, K., M. Kantcheva and D. Klissurski, 1996. *J. Chem. Soc., Faraday Trans.*, 92: 4595.
35. Itho, Y., S. Nishiyama, S. Tsuruya and M.J. Masai, 1994. *Phys. Chem.*, 98: 960.
36. Millar, G.J., C.H. Rochester and K.C. Waugh, 1992. *J. Chem. Soc., Faraday Trans.*, 88: 1477.
37. Bijsterbosh, W.J., F. Kapteigin and A. Moulijn, 1992. *J. Mol. Catal.*, 74: 193.
38. Busca, G., 1987. *J. Mol. Catal.*, 43: 225.
39. Ghiotti, G., F. Bocuzzi and A. Chiorino, 1985. *Stud. Surf. Sci. Catal.*, 21: 235.
40. Hadjiivanov, K., L. Dimitrov, 1999. *Micropor. Mesopor. Mater.*, 27: 49.
41. Hadjiivanov, K., H. Knozinger, 2000. *J. Catal.*, 191: 480.
42. Marta, G., R. Oculi, L. Marchese, G. Genti and S. Coluccia, 2002. *Catal. Today.*, 73: 83.